SCORING OF BREAST TISSUE MICROARRAY SPOTS THROUGH ORDINAL REGRESSION

Telmo Amaral, Stephen McKenna
School of Computing, University of Dundee, Dundee, U.K.

Katherine Robertson and Alastair Thompson
School of Medicine, University of Dundee, Dundee, U.K.

Keywords: Breast tissue microarrays, Scoring, Immunohistochemistry, Ordinal regression.

Abstract: Breast tissue microarrays (TMAs) facilitate the study of very large numbers of breast tumours in a single histological section, but their scoring by pathologists is time consuming, typically highly quantised, and not without error. This paper compares the results of different classification and ordinal regression algorithms trained to predict the scores of immunostained breast TMA spots, based on spot features obtained in previous work by the authors. Despite certain theoretical advantages, Gaussian process ordinal regression failed to achieve any clear performance gain over classification using a multi-layer perceptron. The use of the entropy of the posterior probability distribution over class labels for avoiding uncertain decisions is demonstrated.

1 INTRODUCTION

Tissue microarrays (TMAs) are a high-throughput technique proposed by Kononen (Kononen et al., 1998), to facilitate the study of large numbers of tissue samples on a single histological section; a TMA section contains hundreds of small spots of tissue arranged in a grid-pattern. TMAs are now extensively utilised in the study of cancers. TMAs are constructed by taking cylindrical biopsies (named cores) from donor blocks of formalin fixed wax embedded tissue (tumour or normal) and inserting them into a recipient wax block in a grid arrangement. Sections of the TMA block are cut and provide targets for parallel in situ detection of DNA, RNA, and protein targets in each specimen on the array. Every TMA section contains an array of spots of tissue, each spot being a section of one of the cores previously inserted into the microarray block. Consecutive sections allow the rapid analysis of hundreds of molecular markers in the same set of specimens on only a few histological sections. Camp (Camp et al., 2000) concluded that two cores per patient are sufficient to adequately represent the expression of three common antigens in invasive breast carcinoma.

Immunohistochemistry is carried out to detect protein expression in the tissue spots. For example,

antibodies directed against progesterone receptor can be used to detect nuclear expression of progesterone receptor in breast tumours. Once immunohistochemistry is carried out, the assessment by pathologists of the stained breast TMA sections starts with the classification of each tissue spot. In our experience, the spots are usually one of several types, namely: tumour, normal, stroma, fat, blood, or invalid (no spot present or spot un-assessable). This initial classification must be carried out prior to assessing the immunostaining (level of expression of the protein of interest, e.g. progesterone receptor) due to the fact that the donor cores embedded in the TMA are not always homogeneous throughout their length; there may be tumour in the top third of the core, but the remainder of the core may be stroma. Therefore, to ensure correct analysis, each tissue spot on the TMA section should first be classified as to the type of tissue present. The degree of immunostaining is then assessed and assigned a score. Once all of the spots have been scored, the scores can be compared. Applying this procedure to breast TMA sections incorporating large numbers of tissue samples is time consuming and suffers from inter- and intra-observer variability, perceptual errors, and severe quantisation that leads to the loss of potentially valuable information. Thus, there is strong motivation for the development of au-

tomated methods for quantitative analysis of breast TMA image data.

Most of the published work on automated "ranking" of breast tissue sections aims not at predicting immunohistochemical scores, but rather at distinguishing between different Bloom-Richardson grades, given tissue sections stained solely with Hematoxylin & Eosin. Petushi (Petushi et al., 2006) used supervised learning (namely linear, quadratic, neural network, and decision tree classifiers) to distinguish low, intermediate, and high grades of histology slides, based on tissue texture parameters derived from spatial information on cell nuclei distribution. Axelrod (Axelrod et al., 2008) performed step-wise forward Cox regressions with clinical and pathological factors and image features describing nuclear morphometry, densitometry, and texture, to distinguish low, intermediate, and high worst grades. More recently, Doyle (Doyle et al., 2008) used a support vector machine (SVM) to distinguish low and high grades from digitised histopathology, based on textural and nuclear architecture features. Additional recent work on nuclear grading has been published by Chapman (Chapman et al., 2007), Dalle (Dalle et al., 2008), and Zhang (Zhang et al., 2008). In contrast, Kostopoulos (Kostopoulos et al., 2007) applied k-nearest neighbour weighted votes classification to colour-textural features, in order to predict the oestrogen receptor's (ER) positive status of biopsy images, traditionally assessed via a scoring protocol that takes into account the percentage of epithelial nuclei that are immunopositive.

In this paper, we compare the results of ordinal regression and classification algorithms trained to predict the immunoscores of breast TMA spots. Ordinal regression differs from classification in that the existence of an order between the different categories is taken into account. So, in the prediction of tumour scores, ordinal regression should in principle achieve better results than classification. We trained neural network classifiers and ordinal regression algorithms based on Gaussian processes to predict the Quickscores (Detre et al., 1995) of breast TMA spots subjected to progesterone receptor immunohistochemistry which results in nuclear staining in positive cases. A Quickscore is composed of two integer values, namely a value between 0 and 6 that estimates the proportion of epithelial nuclei that are immunopositive, and a value between 0 and 3 that estimates the strength of staining of those nuclei (these values will henceforth be referred to as QSP and QSS, respectively). In our experiments, each spot is characterised by two features obtained in previous work by the authors, derived from colour and texture features

of pixels, as summarised in section 2.

The remainder of this paper is organised as follows. Section 3 provides an overview of the data and algorithms. Section 4 describes the experiments carried out and presents their results. Section 5 discusses the results and section 6 presents some conclusions and recommendations.

2 PREVIOUS WORK

Our previous work included the classification of breast-TMA spots into two classes, as to the presence or absence of immunopositive epithelial nuclei (regardless of the type of spot) (Amaral et al., 2008). The analysed data consisted of 110 spots (2 for each of 55 participants) subjected to progesterone-receptor (PR) nuclear staining and whose immunostates (positive or negative) were assigned by a pathologist. In addition, the contours of several hundred epithelial nuclei were marked within randomly selected sub-regions and labelled as immunopositive or negative. In a first stage, the pixels within annotated sub-regions were used to estimate the likelihoods of RGB and differential invariant features (computed for two scales up to the 2nd order) for three classes, namely: epithelial positive, epithelial negative, and background. Assuming these features to be independent, their likelihoods were then used to classify the pixels of whole spots into the three considered classes, using Bayes' rule. In a second stage, the previously classified pixels were used to compute features for each spot that aimed to formalise the two Quickscore values assigned by pathologists. A generalised linear model (GLM) was then trained to classify spots as to their immunostate, based on the two computed features. A leave-2-out experiment was carried out, in order to assess the ability of the system to deal with data from new participants. Different combinations of features were tested, leading to the conclusion that the use of differential invariants in addition to colour yielded a small improvement in accuracy. The most favourable combination of features resulted in a correct-classification rate of 84%.

3 MATERIALS AND METHODS

3.1 Data

The data used in this work consist of two features (extracted as described previously in section 2) characterising each of 190 breast TMA spots of normal

or tumour tissue subjected to progesterone receptor (PR) nuclear staining, along with the Quickscore values assigned to those spots by a pathologist. The digitised TMA slides originate from the National Cancer Research Institute's Adjuvant Breast Cancer (ABC) Chemotherapy Trial (Adjuvant Breast Cancer Trials Collaborative Group, 2007).

3.2 Algorithms

Two types of neural networks were trained to classify spots into their QSP and QSS values, namely single-layer networks (also called generalised linear models, or GLMs) and two-layer networks (also called multi-layer perceptrons, or MLPs) (Bishop, 2006). The GLMs were trained through the iterated re-weighted least squares (IRLS) algorithm. The learning algorithm used with the MLPs was scaled conjugate-gradients (SCG) optimisation. For both types of network, softmax was chosen as the activation function. The Netlab (Nabney, 2002) implementations of the GLM and the MLP were used.

For the prediction of QSP and QSS values through ordinal regression, we employed the Gaussian process techniques reported by Chu (Chu and Ghahramani, 2005), briefly summarised in the following. Considering a data set composed of n samples, where the ith sample is a pair of input vector $x_i \in R^d$ and target $y_i \in \{1, 2, ..., r\}$ (without loss of generality). Gaussian processes assume each x_i to be associated with an unobservable latent function $f(x_i) \in R$ (a zero-mean random variable), on which the ordinal variable y_i in turn depends. The process is specified by the covariance matrix for the set of functions, whose elements can be defined by Mercer kernel functions. In this work, we used two types of kernel, namely a linear kernel and a Gaussian kernel, as defined in equations 1 and 2, respectively.

$$Cov[f(x_i), f(x_j)] = \kappa_o \sum \kappa_a x_i^\varsigma x_j^\varsigma \qquad (1)$$

$$Cov[f(x_i), f(x_j)] = \kappa_o exp(-\frac{\kappa_a}{2} \sum_{\varsigma=1}^{d} (x_i^\varsigma - x_j^\varsigma)^2) \quad (2)$$

Every Gaussian process has a number of hyper-parameters that need to be optimised, such as κ_o and κ_a in the formulas above. In this work, for each type of kernel, two Bayesian techniques were used for hyper-parameter learning, here referred to simply as maximum *a posteriori* estimate (MAP) and expectation propagation (EP). We used the Gaussian process algorithms made available by Chu (Chu and Ghahramani, 2005).

Along with the predicted score for each spot, both the classification and ordinal regression algorithms

output r real values that can be interpreted as the posterior probabilities of the spot belonging to each score. As discussed later in section 5, this type of output proved to be useful.

The batch code used to run the experiments and process their results was implemented in Matlab.

4 EXPERIMENTS AND RESULTS

Leave-one-out experiments were carried out to predict the QSP and the QSS values of the 190 available spots, for the classification and ordinal regression algorithms described previously in section 3. For each value type (QSP and QSS), two types of experiment were carried out. In the first case, the models were trained to predict raw Quickscore values. These experiments are referred to as *Raw* in table 1. In the second case, the models were trained to predict collapsed Quickscore values, obtained from the raw values as shown in equations 3 and 4. These experiments are referred to as *Collapsed* in table 1. In addition, the raw predicted values resulting from the first case were collapsed *a posteriori*, so as to be comparable with those resulting from the second case. These modified results are referred to as *Raw c.a.p.* in table 1.

$$v_{QSP.collapsed} = \begin{cases} 0 & \text{if } v_{QSP.raw} = 0 \\ 1 & \text{if } v_{QSP.raw} \in \{1, 2\} \\ 2 & \text{if } v_{QSP.raw} \in \{3, 4\} \\ 3 & \text{if } v_{QSP.raw} \in \{5, 6\} \end{cases} \quad (3)$$

$$v_{QSS.collapsed} = \begin{cases} 0 & \text{if } v_{QSS.raw} = 0 \\ 1 & \text{if } v_{QSS.raw} \in \{1, 2\} \\ 2 & \text{if } v_{QSS.raw} = 3 \end{cases} \quad (4)$$

Chu (Chu and Ghahramani, 2005) reported results for various data sets and algorithms, to support the comparison between algorithms. The result reported for each experiment consists of the mean absolute error (i.e. the average deviation of the prediction from the true target) over all test samples, along with the standard deviation of *partial* mean absolute errors. Each partial error is computed over the test samples included in a given random partition of the data. For each data set, a number of random partitions is defined. A standard deviation computed in this way, however, has the disadvantage of depending on the partitioning of the data (specifically, on the number of test samples per partition). In our work, for each experiment, we chose to compute the mean and standard deviation of the absolute error over all samples. These values are presented in table 1, the best results on each row being typed in boldface.

Table 1: Means and standard deviations of the absolute errors yielded by the various experiments.

Target QS value		Algorithm					
		Netlab		Gaussian process ordinal regression			
		GLM	MLP	MAP		EP	
				Lin.	Gau.	Lin.	Gau.
P	Raw	1.400 ±1.677	0.926 ±1.215	1.126 ±1.397	0.921 ±1.172	0.900 ±1.129	**0.888 ±1.175**
P	Raw c.a.p.	0.774 ±0.935	0.516 ±0.733	0.626 ±0.805	0.537 ±0.702	**0.500 ±0.680**	0.503 ±0.698
P	Collapsed	0.684 ±0.870	0.432 ±0.677	0.579 ±0.757	**0.426 ±0.619**	0.463 ±0.639	**0.426 ±0.611**
S	Raw	0.937 ±1.097	**0.763 ±0.988**	0.937 ±1.106	0.784 ±1.003	0.800 ±1.025	0.779 ±0.994
S	Raw c.a.p.	0.674 ±0.727	**0.547 ±0.655**	0.663 ±0.729	0.558 ±0.662	0.568 ±0.677	0.553 ±0.655
S	Collapsed	0.589 ±0.626	0.495 ±0.589	0.526 ±0.606	0.495 ±0.561	**0.489 ±0.589**	**0.489 ±0.561**

For each experiment, besides the values reported in table 1, a confusion matrix was computed. The matrices for some of the experiments are shown in Table 2.

a) QSS Collapsed, EP Gau
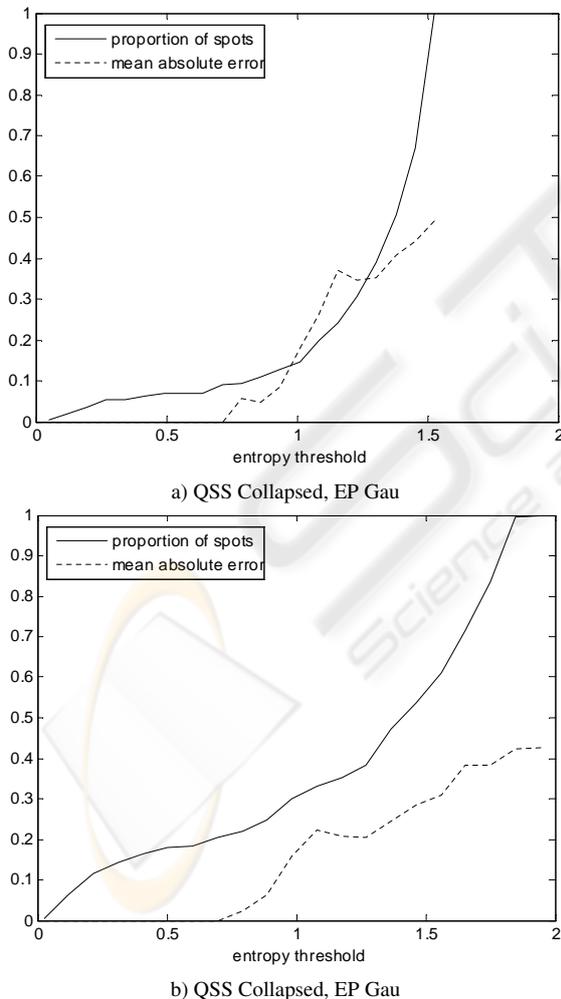

b) QSS Collapsed, EP Gau

Figure 1: Fraction of processed spots, and mean absolute error over those spots, versus confidence threshold, for two of the experiments (lower entropy means higher confidences.

As mentioned previously in section 3, all of the employed algorithms output, along with each prediction, a posterior probability distribution over the r targets. The entropy of a posterior distribution can be used as a simple measure of classification or ordinal regression confidence (the lower the entropy, the higher the confidence). For two of the experiments, figure 1 shows the fraction of test spots that can be predicted below a given entropy threshold. Also shown is the mean absolute error computed over each fraction of spots.

5 DISCUSSION

Models trained to predict collapsed Quickscore values consistently yielded better mean absolute errors than models trained to predict the same Quickscores in raw format (collapsed only *a posteriori* for the purpose of comparison). This difference in quality of the results was also reflected in the confusion matrices. All matrices for the prediction of raw Quickscores (QSPs or QSSs, regardless of the algorithm) showed one or two middle targets with zero predictions, but this effect was not observable in the matrices for the prediction of collapsed Quickscores. To illustrate this, tables 2(a) and (b) show the matrices for the prediction of raw and collapsed QSPs, respectively, via the EP algorithm with Gaussian kernel; and tables 2(c) and (d) show the matrices for the prediction of QSSs via MLP and EP with Gaussian kernel, respectively. This may indicate a lack of training examples for middle targets, or inadequacy of the features used to characterise TMA spots, or even that the number of scoring ordinals used in practice is excessive.

The GLM algorithm performed poorly. Besides yielding the highest mean absolute error in every experiment, the prediction of collapsed QSPs yielded a confusion matrix that showed a middle target with no predictions, something that did not happen with any

Table 2: Confusion matrices for some of the experiments.

(a) QSP Raw, EP, Gau

Test	Predicted						
	0	1	2	3	4	5	6
0	65	00	04	00	01	00	00
1	16	00	02	00	00	00	00
2	13	00	08	00	03	00	01
3	03	00	08	00	04	03	00
4	04	00	04	00	04	04	02
5	03	00	03	00	02	01	07
6	00	00	01	00	00	04	17

(b) QSP Collapsed, EP, Gau.

Test	Predicted			
	0	1	2	3
0	59	11	02	00
1	21	15	06	01
2	03	09	18	07
3	01	03	06	28

(c) QSS Raw, MLP

Test	Predicted			
	0	1	2	3
0	68	00	00	04
1	15	00	00	16
2	08	00	00	29
3	13	00	02	35

(d) QSS Collapsed, EP, Gau

Test	Predicted		
	0	1	2
0	52	20	00
1	16	28	24
2	06	21	23

(e) QSP Collapsed, GLM

Test	Predicted			
	0	1	2	3
0	65	00	03	04
1	39	00	02	02
2	19	00	09	09
3	05	00	05	28

other algorithm. This matrix is shown in table 2(e).

Ordinal regression with EP and Gaussian kernel could be said to be the best algorithm, based solely on the mean absolute errors. It yielded an error that was always either the lowest or very close to the lowest. However, the large values of the absolute error's standard deviation shown in table 1 seem to render a comparison between algorithms inconclusive.

It should also be noted that the MLP algorithm performed surprisingly well, when compared with the ordinal regression methods. This suggests that further research to improve the ordinal regression method is needed, given the expectation that formulating the tissue scoring problem as ordinal regression should represent an advantage over classification. A possibility would be to investigate modifications to the ordinal regression algorithms that could model the way in which pathologists mislabel the ground-truth. The MLP also consumed a computational time per TMA spot that is is at least one order of magnitude below that taken by the ordinal regression (tenths of second versus several seconds).

As the entropy threshold set on the predictions was decreased (i.e., as the minimum confidence threshold is increased), the mean absolute error tended to decrease, as exemplified in Figures 1(a) and (b). This suggests that it is possible to automatically process, with quite low mean errors, reasonable fractions of spots that are more unequivocal, while identifying the more difficult spots that cannot dispense with human assessment.

6 CONCLUSIONS AND RECOMMENDATIONS

This paper compared the results of ordinal regression and classification algorithms trained to predict the scores of breast tissue sections. Purely in terms of mean absolute errors, ordinal regression via EP with Gaussian kernel yielded the best results in most experiments, but the MLP classifier's performance is practically at the same level. The reasons behind this should be further investigated. In turn, GLM was found to perform poorly. Models trained to predict collapsed ordinal targets achieve considerably better results than models trained to predict raw targets (collapsed only *a posteriori* for comparison). It would be interesting to further investigate this limitation, too.

By setting confidence thresholds, it should be possible to use the methods discussed in this paper to process reasonable fractions of spots with low mean absolute errors. Future work should also investigate how to take into account the costs of different kinds of error (e.g. predicting a score of 2 as 1 should in principle have a lower cost than predicting a 1 as 0), and build those into the ordinal regression model.

REFERENCES

Adjuvant Breast Cancer Trials Collaborative Group (2007). Polychemotherapy for early breast cancer: Results from the international adjuvant breast cancer

chemotherapy randomized trial. *Journal of the National Cancer Institute*, 99(7):506–515.

Amaral, T., McKenna, S., Robertson, K., and Thompson, A. (2008). Classification of breast-tissue microarray spots using colour and local invariants. In *IEEE International Symposium on Biomedical Imaging: From Nano to Macro*, pages 999–1002, Paris, France. IEEE.

Axelrod, D., Miller, N., Lickley, H., Qian, J., Christens-Barry, W., Yuan, Y., Fu, Y., and Chapman, J. (2008). Effect of Quantitative Nuclear Image Features on Recurrence of Ductal Carcinoma In Situ (DCIS) of the Breast. *Cancer Informatics*, 4:99–109.

Bishop, C. M. (2006). *Pattern Recognition and Machine Learning (Information Science and Statistics)*. Springer-Verlag New York, Inc., Secaucus, NJ, USA.

Camp, R., Charette, L., and Rimm, D. (2000). Validation of tissue microarray technology in breast carcinoma. *Laboratory Investigation*, 80(12):1943–1949.

Chapman, J., Miller, N., Lickley, H., Qian, J., Christens-Barry, W., Fu, Y., Yuan, Y., and Axelrod, D. (2007). Ductal carcinoma in situ of the breast (DCIS) with heterogeneity of nuclear grade: prognostic effects of quantitative nuclear assessment. *BMC Cancer*, 7:174.

Chu, W. and Ghahramani, Z. (2005). Gaussian processes for ordinal regression. *Journal of Machine Learning Research*, 6:1019–1041.

Dalle, J., Leow, W., Racoceanu, D., Tutac, A., and Putti, T. (2008). Automatic Breast Cancer Grading of Histopathological Images. In *International Conference of the IEEE Engineering in Medicine and Biology Society*, pages 3052–3055.

Detre, S., Saccani Jotti, G., and Dowsett, M. (1995). A "quickscore" method for immunohistochemical semi-quantitation: validation for oestrogen receptor in breast carcinomas. *Journal of Clinical Pathology*, 48(9):876–878.

Doyle, S., Agner, S., Madabhushi, A., Feldman, M., and Tomaszewski, J. (2008). Automated grading of breast cancer histopathology using spectral clustering with textural and architectural image features. In *IEEE International Symposium on Biomedical Imaging: From Nano to Macro*, pages 496–499. IEEE.

Kononen, J., Bubendorf, L., Kallionimeni, A., Brlund, M., Schraml, P., Leighton, S., Torhorst, J., Mihatsch, M., Sauter, G., and Kallionimeni, O. (1998). Tissue microarrays for high-throughput molecular profiling of tumor specimens. *Nature Medicine*, 4(7):844–847.

Kostopoulos, S., Cavouras, D., Daskalakis, A., Bougioukos, P., Georgiadis, P., Kagadis, G., Kalatzis, I., Ravazoula, P., and Nikiforidis, G. (2007). Colour-Texture based image analysis method for assessing the Hormone Receptors status in Breast tissue sections. In *International Conference of the IEEE Engineering in Medicine and Biology Society*, pages 4985–4988. IEEE.

Nabney, I. (2002). *NETLAB: algorithms for pattern recognition*. Springer-Verlag, New York.

Petushi, S., Garcia, F., Haber, M., Katsinis, C., and Tozeren, A. (2006). Large-scale computations on histology images reveal grade-differentiating parameters for breast cancer. *BMC Medical Imaging*, 6:14.

Zhang, J., Petushi, S., Regli, W., Garcia, F., and Breen, D. (2008). A study of shape distributions for estimating histologic grade. In *International Conference of the IEEE Engineering in Medicine and Biology Society*, pages 1200–1205.